Supplemental Material can be found at:
http://www.jbc.org/cgi/content/full/M708621200/DC1

THE JOURNAL OF BIOLOGICAL CHEMISTRY VOL. 283, NO. 8, pp. 5099–5109, February 22, 2008
© 2008 by The American Society for Biochemistry and Molecular Biology, Inc. Printed in the U.S.A.

Solitary and Repetitive Binding Motifs for the AP2 Complex α-Appendage in Amphiphysin and Other Accessory Proteins*[S]

Received for publication, October 17, 2007, and in revised form, November 2, 2007 Published, JBC Papers in Press, November 6, 2007, DOI 10.1074/jbc.M708621200

Lene E. Olesen[‡1], Marijn G. J. Ford[‡1,2], Eva M. Schmid[‡1], Yvonne Vallis[‡], M. Madan Babu[‡], Peter H. Li[‡3], Ian G. Mills[‡4], Harvey T. McMahon[‡5], and Gerrit J. K. Praefcke[§6]

From the [‡]Laboratory of Molecular Biology, Medical Research Council, Neurobiology Division, Hills Road, Cambridge CB2 2QH, United Kingdom and the [§]Center for Molecular Medicine Cologne, Institute for Genetics, Zülpicher Strasse 47, 50674 Cologne, Germany

Adaptor protein (AP) complexes bind to transmembrane proteins destined for internalization and to membrane lipids, so linking cargo to the accessory internalization machinery.This machinery interacts with the appendage domains of APs, which have platform and β-sandwich subdomains, forming the binding surfaces for interacting proteins. Proteins that interact with the subdomains do so via short motifs, usually found in regions of low structural complexity of the interacting proteins. So far, up to four motifs have been identified that bind to and partially compete for at least two sites on each of the appendage domains of the AP2 complex. Motifs in individual accessory proteins, their sequential arrangement into motif domains, and partial competition for binding sites on the appendage domains coordinate the formation of endocytic complexes in a temporal and spatial manner. In this work, we examine the dominant interaction sequence in amphiphysin, a synapse-enriched accessory protein, which generates membrane curvature and recruits the scission protein dynamin to the necks of coated pits, for the platform subdomain of the α-appendage. The motif domain of amphiphysin1 contains one copy of each of a D*X*(F/W) and F*X*D*X*F motif. We find that the F*X*D*X*F motif is the main determinant for the high affinity interaction with the α-adaptin appendage. We describe the optimal sequence of the F*X*D*X*F motif using thermodynamic and structural data and show how sequence variation controls the affinities of these motifs for the α-appendage.

Clathrin-mediated endocytosis is the process whereby proteins and lipids destined for internalization from the plasma membrane are packaged into vesicles with the aid of a clathrin coat. Purified coated vesicles from brain contain three major components as follows: clathrin, AP180, and AP2 complexes (1–3). Clathrin triskelia oligomerize to provide the scaffold around the forming vesicle (and can form similar cages in solution (4)). With its terminal domain, clathrin interacts with other endocytic proteins, including the AP2[7] complex, AP180, epsin, disabled-2 (Dab2), and amphiphysin. These interactions are mediated via short motifs; for example, clathrin binds to amphiphysin through motifs such as LLDLD or PW*XX*W (5, 6). Because oligomeric clathrin presents an array of binding sites for these motifs, it serves as a network hub, organizing binding partners within the lattice. The AP complexes, as well as many accessory proteins and alternative cargo adaptors such as AP180, Dab2, epsin, and amphiphysin, recruit clathrin to PtdIns(4,5)P_2-rich areas in the membrane and promote its polymerization into a lattice. Because of its significant number of interaction partners, another key hub in the endocytic interactome is the AP2 complex (7–9). It consists of four subunits (α, β2, μ2, and σ2) and forms a stable heterotetramer in solution (10). Using electron microscopy it was shown that the AP2 complex can be subdivided into the following: (i) a trunk domain, which interacts with cargo proteins and PtdIns(4,5)P_2, and (ii) two appendage domains made from the C termini of the α- and β-subunits, which interact with a large number of accessory proteins by binding to short motifs in these proteins. For example, the α-adaptin appendage binds to D*X*(F/W), F*X*D*X*F, W*XX*(F/W), and F*XX*F*XX*L motifs (7, 11–16). These can be highly clustered in motif domains of the accessory proteins

* This work was supported by a fellowship from the Danish Research Academy (to L. E. O.), a research fellowship from Downing College, Cambridge, UK (to M. G. J. F.), a fellowship from the Austrian Academy of Science (to E. M. S.), and a Marie Curie Fellowship from European Union Contract HPMF-CT-2000-01086 (to G. J. K. P.). The costs of publication of this article were defrayed in part by the payment of page charges. This article must therefore be hereby marked "*advertisement*" in accordance with 18 U.S.C. Section 1734 solely to indicate this fact.

The atomic coordinates and structure factors (code 2vj0) have been deposited in the Protein Data Bank, Research Collaboratory for Structural Bioinformatics, Rutgers University, New Brunswick, NJ (http://www.rcsb.org/).

[S] The on-line version of this article (available at http://www.jbc.org) contains a supplemental table.

[1] These authors contributed equally to this work.

[2] Present address: Section of Molecular and Cellular Biology, University of California, Davis, CA 95616.

[3] Present address: Depts. of Ophthalmology and Physiology, University of California, San Francisco, 10 Koret Way, San Francisco, CA 94143-0730.

[4] Present address: CRUK Uro-Oncology Research Group, Cambridge Cancer Research Institute, Robinson Way, Cambridge, CB2 0RE, UK.

[5] To whom correspondence may be addressed. Tel.: 44-1223-402311; Fax: 44-1223-402310; E-mail: hmm@mrc-lmb.cam.ac.uk.

[6] To whom correspondence may be addressed. Tel.: 49-221-470-1561; Fax: 49-221-470-6749; E-mail: gpraefck@uni-koeln.de.

[7] The abbreviations used are: AP2, adaptor protein complex 2; Amph, amphiphysin; AP180, adaptor protein of 180 kDa; BAR, Bin2/amphiphysin/Rvs; CALM, clathrin assembly lymphoid myeloid leukemia protein; Dab2, Disabled 2; Eps15, epidermal growth factor receptor pathway substrate 15; epsin, Eps15-interacting protein; GST, glutathione *S*-transferase; HIP1, Huntingtin interacting protein 1; ITC, isothermal titration calorimetry; PLAA, phospholipase A2 activator; PDB, Protein Data Bank; SH, Src homology; DTT, dithiothreitol; PtdIns(4,5)P_2, phosphatidylinositol 4,5-bisphosphate.

Downloaded from www.jbc.org at MRC Lab of Molecular Biology on October 18, 2008

where they are also frequently found close to clathrin-binding motifs. The appendage domains are connected to the trunk domain by flexible linkers, which lack a defined secondary structure in solution.

Although the AP2 appendages are only 16% identical in terms of their sequences, they are structurally very similar (12, 17). We and others have previously proposed that both the α- and β2- appendage domains bind to D*X*(F/W) motifs in accessory proteins (7, 8, 12, 18). The D*X*(F/W) motifs on accessory proteins are often found in proline-rich regions. For example, rat epsin1 has nine DPW motifs, and the majority of these are found in a proline-rich stretch of 105 amino acids, a region that by CD spectroscopy has no obvious structure (19). Human Eps15 contains 15 DPF and two other D*X*F motifs in a stretch of 230 amino acids. These motifs may allow clustering of the AP2 complexes at the endocytic assembly zones and enhance the binding to PtdIns(4,5)P_2-containing membranes (8, 20). D*X*(F/W) motifs bind to sites on the platform subdomains of the appendages, centered around a hydrophobic pocket (Trp-840 in α; Trp-841 in β2) (12, 17) in a tight turn conformation (18). In the study by Brett *et al.* (18), the authors also found a secondary binding site for DPW motifs on the β-sandwich subdomain of the α-appendage. More importantly, they found that an FEDNF peptide from amphiphysin binds to the top of the α-appendage using the site around Trp-840 but in a different conformation by inserting the first Phe residue into the hydrophobic pocket. It was therefore proposed that F*XDXF* is a general high affinity binding motif for the α-adaptin appendage. Recently, a fourth binding motif for the α-adaptin appendage has been identified in the proteins NECAP, stonin, synaptojanin, connecdenn, and others (15, 21–23). The binding motif consensus W*XX*(F/W) resembles the second clathrin-binding motif PW*XX*W, but the proline residue seems to mediate the discrimination between the binding partners.

Recently, we showed how multiple adaptin-binding motifs provide an avidity effect where the overall apparent affinities for AP2 complexes will depend on the type, number, and spacing of binding motifs as well as the clustering of available appendage domains (7, 8). The unclustered cytoplasmic AP2 complex has single α- and β2-appendage domains, whereas in the coated pit there will be many such domains from clustered AP2 complexes. However, when AP2 complexes are bound to polymerized clathrin, the β2-adaptin appendage domain is predicted to be largely occupied by clathrin, and steric hindrance is thought to exclude most accessory proteins. AP2 complexes at the edge of coated pits, where there is a lower concentration of clathrin, are predicted to still be free to bind the full complement of accessory proteins. The complement of accessory proteins bound to AP2 complexes in the cytosol is again proposed to be different (8). Thus, Eps15 has been shown to be restricted to the edges of a nascent coated pit as its interaction with AP2 adaptors is displaced by clathrin (24, 25). A similar scenario applies for amphiphysin1, which contains an F*XDX*F, a DPF, and a DLW motif, the latter two of which overlap with two clathrin-binding motifs (Fig. 1*A*). As a result, amphiphysin would also be primarily localized to the edges of the invaginating pit, ending up at the neck of the nascent vesicle. This would be a convenient way for amphiphysin to ensure that its C-terminal SH3 domain delivers dynamin to the neck of a coated pit, whereas the N-terminal BAR domain of amphiphysin binds to PtdIns(4,5)P_2 and generates vesicle curvature in the membrane (26). The BAR domain is also responsible for the dimerization of amphiphysin, which increases the efficiency of binding to the proline-rich domain in dynamin.

Mammals have two isoforms of amphiphysin (27), amphiphysin1 and -2 (Amph1 and -2). There is low sequence conservation of the domain in which these motifs occur. However, only the FEDNF motif is well conserved (as an FEDAF in Amph2), whereas the DPF motif is EPL in Amph2. The muscle form of Amph2 (bridging integrator-1/Bin1) and amphiphysin in *Drosophila* have no D*X*F motifs in this region. In muscle, the protein is associated with T-tubule formation and not with clathrin/adaptor endocytosis. Accordingly, in *Drosophila* deletion of the protein gives a muscle weakness phenotype and a defect in T-tubule formation (28, 29). Thus, the presence of a clathrin/adaptor-binding domain targets amphiphysin for function in clathrin-mediated endocytosis.

The selection of amphiphysin1 to study the individual contributions of different binding motifs for α-adaptin offers several advantages over other accessory proteins such as epsin1, Eps15, or AP180. First, amphiphysin is highly specific for the α-adaptin appendage and binds to other adaptins weakly (17), thereby avoiding avidity effects from interactions with other AP components. Second, amphiphysin contains single copies of the possible adaptin-binding motifs, which limits interference by avidity effects and makes mutagenesis straightforward. These motifs are separated by 20–30 residues, which should be distant enough to avoid steric hindrance. Finally, despite the low number of motifs, the binding has a high affinity and amphiphysin is a major AP2-binding partner with an essential biological function. Using a combination of thermodynamic, biochemical, and structural observations, we show that the F*XDX*F motif is the main determinant for the high affinity binding to the α-adaptin appendage. Moreover, we define the optimal F*XDX*F motif and use these data to explain the observed binding characteristics of other F*XDX*F- and D*X*(F/W)-containing accessory proteins.

EXPERIMENTAL PROCEDURES

Constructs and Protein Expression—The α-adaptin appendage domain (residues 701–938) and the appendage-plus hinge domain (residues 653–938), the human β2-adaptin appendage domain (residues 701–937), rat amphiphysin1AB (Amph1AB; residues 1–378), and rat amphiphysin2AB (Amph2AB; residues 1–422) were expressed as N-terminal glutathione *S*-transferase (GST) fusion proteins (in pGex4T2) in BL21 cells following overnight isopropyl 1-thio-β-D-galactopyranoside induction at 22 °C. All GST fusion proteins were purified from bacterial extracts by incubation with glutathione-Sepharose beads, followed by extensive washing with 20 mM HEPES, pH 7.4, 150 mM NaCl, 1 mM DTT. The fusion proteins were cleaved by incubation for 2 h with thrombin and further purified by passage over a Q-Sepharose column. For isothermal titration calorimetry (ITC) experiments, the protein was additionally passed down a Superdex 75 gel filtration column and dialyzed into 100 mM HEPES, pH 7.4, 50 mM NaCl, 2 mM DTT.

Downloaded from www.jbc.org at MRC Lab of Molecular Biology on October 18, 2008

GST-Amph1AB was not cleaved to prevent degradation of the protein. Myc-tagged proteins (in pCMV-myc) were used for expression in COS-7 fibroblasts. The appendage domain of human β2-adaptin (residues 701–937) was expressed in BL21 cells as an N-terminal His_6 fusion protein (in pET-15b) and purified by passage over nickel-nitrilotriacetic acid, followed by Q-Sepharose and gel filtration chromatography. Mutations were generated by PCR using overlapping primers incorporating the base pair changes.

Transfections, Antibodies, and Cell Extracts—COS-7 cells were transfected using GeneJuice (Novagen) according to the manufacturer's protocol. Overexpressed Amph1AB was detected using a polyclonal anti-Myc antibody (Cell Signaling, green in merged images). The endogenous AP2 complex was detected using a Sigma monoclonal antibody (red in merged images). Cells were imaged using a Bio-Rad Radiance confocal system. For extracts, two 70-mm dishes of COS cells were scraped in 1 ml of phosphate-buffered saline + 0.1% Triton X-100, or one rat brain was homogenized in 10 ml of phosphate-buffered saline + 0.1% Triton X-100 and cleared by centrifugation.

Pull Downs from COS-7 Cell or Rat Brain Extracts with GST Appendages—For interaction experiments, the extracts described above were incubated with 30–50 μg of GST fusion protein on glutathione-Sepharose beads for 1 h at 4 °C, and then the bead-bound proteins were washed four times with 150 mM NaCl, 20 mM HEPES, pH 7.4, 2 mM DTT, protease inhibitors, and 0.1% Triton X-100. Interaction partners were analyzed by SDS-PAGE and Western blotting. All experiments were repeated three to five times. The α- and δ-adaptin and amphiphysin1 were detected using monoclonal antibodies from BD Biosciences, and β1,2- and γ-adaptin were detected with monoclonal antibodies from Sigma.

Isothermal Titration Calorimetry—Binding of peptides and proteins to α- and β2-adaptin appendage domains was investigated by isothermal titration calorimetry (30) using a VP-ITC (MicroCal Inc.). All experiments were performed in 100 mM HEPES, pH 7.4, 50 mM NaCl, 2 mM DTT at 10 °C unless otherwise stated. The peptides or proteins were injected from a syringe in 40–50 steps up to a 3–4-fold molar excess. The cell contained 1.36 ml of protein solution, and typically the ligand was added in steps of 4–8 μl every 3.5 min. Concentrations were chosen so that the binding partners in the cell were at least 5-fold higher than the estimated dissociation constant, if possible. The ligands in the syringe were again at least 10-fold more concentrated. Titration curves were fitted to the data using ORIGIN (supplied by the manufacturer) yielding the stoichiometry N, the binary equilibrium constant K_a ($= K_d^{-1}$), and the enthalpy of binding ΔH. The entropy of binding ΔS was calculated from the relationship $\Delta G = -RT \cdot \ln K_a$ and the Gibbs-Helmholtz equation. The values were averaged from two to three titrations. Protein concentrations were determined by measuring the A_{280}. Peptides were purchased at >95% purity from the Institute of Biomolecular Sciences, University of Southampton, UK, and weighed on an analytical balance. Where possible, peptide concentrations were verified by measuring A_{280} or A_{257}. The resulting errors on the concentrations are estimated to be <10% for the proteins and the peptides. Unless otherwise stated, the values for the stoichiometry N were within this error region around $N = 1$.

Crystallography and Structure Determination—Co-crystals of α-adaptin appendage and the synaptojanin WV*X*F peptide were grown by hanging-drop vapor diffusion against a reservoir containing conditions centered around 1.2 M ammonium sulfate, 3% isopropyl alcohol, and 0.05 M sodium citrate. Hanging drops were 2 μl and contained 222 μM α-adaptin appendage and 277.5 μM synaptojanin WV*X*F peptide (sequence NPKGWVTFEEEE). Crystals were obtained after incubation for ~1 week at 18 °C. To obtain crystals containing peptides bound to the top side, α-adaptin appendage-WV*X*F co-crystals were soaked in a solution of mother liquor containing amphyphysin1 FEDNFVP peptide. Crystals were cryo-protected by transfer to Paretone-N (Hampton Research) and were flash-cooled in liquid nitrogen. Data to 1.6 Å were collected at 100 K at Station 9.6 SRS Daresbury, UK. Crystals were monoclinic and belonged to space group C2 (a = 146.6 Å, b = 67.3 Å, c = 39.7 Å, β = 94.53°). Data collection statistics are shown in supplemental Table 1. Reflections were integrated using MOSFLM (31) and were scaled using the CCP4 suite of crystallographic software (32). A difference Fourier, calculated using our model of the α-appendage bound to the WV*X*F peptide,[8] revealed beautiful density for the amphiphysin peptide. The model was completed using COOT (33) and O (34) and was refined using REFMAC5 (35). The validated coordinates and structure factors for the crystal structure containing the synaptojanin WV*X*F and the amphyphysin1 FEDNFVP have been deposited in the Protein Data Bank (36) (PDB code 2vj0). Figures were generated using Aesop,[9] and the peptide interaction map was generated using the output from LIGPLOT (37) as a starting point.

RESULTS

The region in amphiphysin1 necessary for binding to the AP2 complex has been mapped to residues 322–340, and binding is enhanced if the region is extended to 322–363 (38). This includes the $FEDNF^{328}$ and the DPF^{359} motifs (Fig. 1*A*). A further extension to include the PW*XX*W had no additional effect on binding. Using isothermal titration calorimetry, we found that a construct from residues 1–378, which forms a dimer because of its N-terminal BAR domain (26), binds to the α-adaptin appendage with an affinity of 1.6 μM but does not interact with the β2-adaptin appendage (Fig. 1*B*). This affinity is very similar to the one measured for the 12-mer DNF-peptide INF**FED**N**F**VPEI (7). In addition, the stoichiometry of the interaction between the α-adaptin appendage and the amphiphysin protein, as well as the DNF 12-mer, is 1:1. A longer construct, residues 1–390, comprising the F*X*D*X*F, DPF, and the PW*XX*W motifs, had a similar affinity, although a contribution of a second very weak binding site becomes visible (data not shown). Thus, the FEDNF in amphiphysin1 is the major determinant for the binding to the α-adaptin appendage.

Adaptor Binding by Amphiphysin via FXDNF and DPF Motifs—We extended these observations by mutagenesis of both motifs sequentially and simultaneously and show that AP2

[8] M. G. J. Ford and G. J. K. Praefcke, unpublished data.
[9] M. Noble, personal communication.

Downloaded from www.jbc.org at MRC Lab of Molecular Biology on October 18, 2008

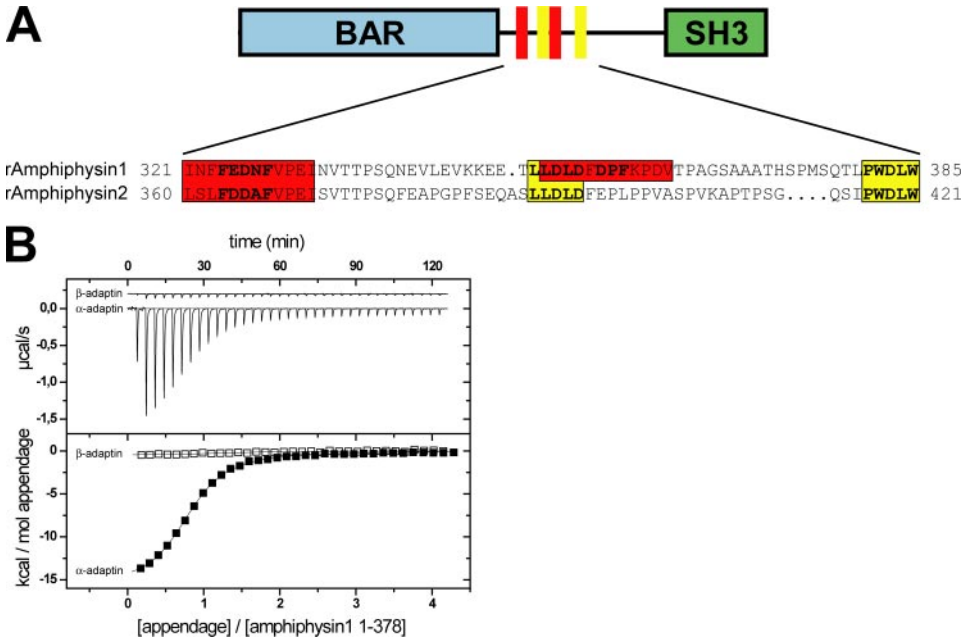

FIGURE 1. **Interaction of amphiphysin with appendage domains.** *A*, schematic representation of the domain architecture of mammalian amphiphysin. The motif domain is located between the N-terminal BAR and the C-terminal SH3 domain. The blow-up shows the sequence conservation between rat amphyphysin1 and -2. *Red blocks* represent the D*X*F motifs that were used as peptides to determine the specificity of the interaction, and *yellow blocks* represent clathrin-binding motifs. *B*, profiles of typical calorimetric titrations of the α-adaptin and β2-adaptin appendage domain into a solution of GST-amphiphysin1 (residues 1–378), at 10 °C (*upper panel*), and the integrated data normalized to the concentration of the appendage domain (*lower panel*). The fit yields a dissociation constant of 1.6 μM, Δ*H* of −16 kcal/mol, and Δ*S* of −30 cal/mol·K.

binding to the DNF motif at residue 326 is stronger than binding to the DPF at residue 357 (Fig. 2*A*). Mutations of both DNF and DPF motifs to SGA are even more effective than the single mutants in disrupting binding. In pulldown experiments from brain and COS-7 cell extracts, α- and β-adaptins follow the same pattern, because they are part of the same complex (AP2). We already know from Fig. 1 that amphiphysin is specific for α-adaptin. There is also no interaction of γ- and δ-adaptins with amphiphysin, showing that AP1 and AP3 complexes in COS-7 extracts do not bind to amphiphysin (Fig. 2*A*). From this it is clear that both motifs contribute to AP2 binding, but there is a clear difference in affinity for the α-adaptin appendage. In Amph2 the FEDAF motif is the major binding sequence for AP2 adaptors (Fig. 2*C*).

Given the strong effect of mutagenesis of the F*X*D*X*F motifs in amphiphysin1 and -2, we tested how well other residues might substitute (Fig. 2, *B* and *C*). The initial surprise was that F*X*DPF does not substitute for F*X*DNF but that F*X*DPW does. The structural basis for this is not clear, but different peptides can bind in different conformations. The FEDNF peptide from amphiphysin and the FKDSF from synaptojanin bind in an extended conformation where the first F in this binds into the pocket formed by Phe-836, Phe-837, and Trp-840 (7, 18). This cannot be the case for most D*X*(F/W) peptides that do not have an equivalent Phe residue, and the proline residue in the DP(F/W) motifs forces the peptide into a loop structure. Binding is also possible when the Asn residue in the FEDNF motif of amphiphysin1 is replaced by Ser, Ala, Asp, or Ile, whereas Gly and Leu abolish the interaction. For amphiphysin2, we looked at a more limited set of substitutions (Fig. 2*C*), but again the change of F*X*DAF to F*X*DPF weakens the interaction. The F*X*D*X*F is the major binding motif of amphiphysins; however, we should be very cautious in extending this observation to other proteins that have other nonconserved residues (see below). An interesting observation was that the presence of the hinge domain of the α-adaptin appendage increased the binding of amphiphysin1 to the top binding site (Fig. 2*D*). This is reminiscent of the interaction of the hinge region of β-adaptin with the clathrin terminal domain. Addition of a peptide derived from the proline-rich region of dynamin did not abolish this effect so that an interaction between a proline-rich stretch in the α-hinge with the SH3 domain of amphiphysin can be ruled out (data not shown).

Use of DXF in Vivo—We and others have shown that overexpression of D*X*F domains can inhibit endocytosis (3, 39–41). In the case of amphiphysin, overexpression of the full-length protein in COS-7 cells inhibits endocytosis of transferrin (27, 38), and this can be rescued by co-expression of dynamin. Thus, part of the inhibitory phenotype is because of sequestration of dynamin. This effect can be mimicked by overexpression of the SH3 domain (42). Given that amphiphysin has a very low affinity for dynamin in solution (100–200 μM) but binds to dynamin very tightly when bound to beads implies that the clustering of amphiphysins results in a strong avidity for dynamin. Thus, if we can prevent the clustering of amphiphysin by blocking the recruitment to sites of endocytosis by mutagenesis of the D*X*F motifs, we should prevent the inhibitory potential of the overexpressed protein. Fig. 3*A* shows that overexpression of WT amphiphysin1 inhibits transferrin uptake and results in a redistribution of AP2 adaptors when compared with nontransfected control cells at the same plane of focus. Point mutants of the DNF and the DPF motifs partially rescue the transferrin uptake inhibition phenotype as well as the adaptor redistribution. The rescue is most efficient with the F*X*DNF+DPF double mutant (Fig. 3*B*). For the single mutants the FEDNF → FESGA protein shows a weaker inhibition of endocytosis than the DPF → SGA version. We conclude that both motifs of amphiphysin are indeed involved in binding AP2 adaptors *in vivo*. Also, as argued above, this experiment underlines that dynamin is recruited to sites of endocytosis by amphiphysin if it is clustered at active zones.

Affinities of FXDXF Motifs—We have shown that DPF peptides have an affinity for the α-adaptin appendage in the range of 100 μM (12). Recently, we found that the F*X*D*X*F peptides from amphiphysin1 and the 170- kDa isoform of synaptojanin have a higher affinity, in the range of 2–20 μM (7). The

Downloaded from www.jbc.org at MRC Lab of Molecular Biology on October 18, 2008

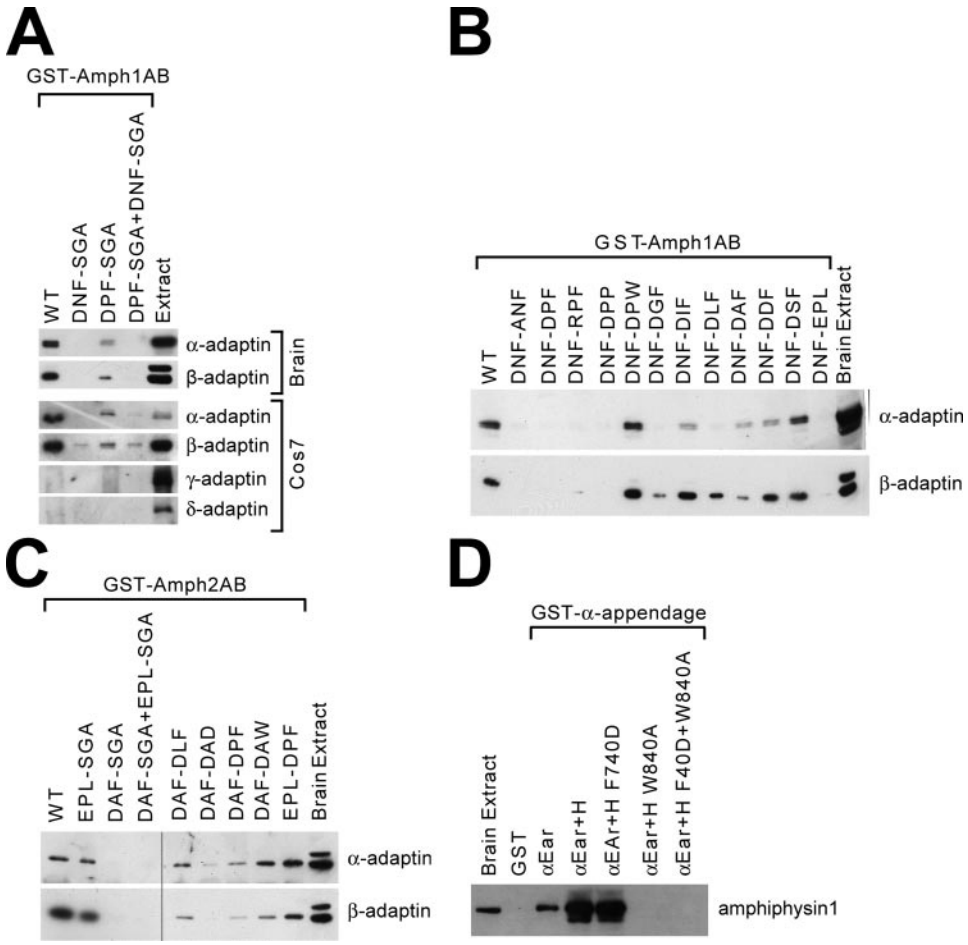

FIGURE 2. **Contributions of the two D*X*F motifs in amphiphysin1 and -2.** *A*, GST fusions of the N-terminal 378 residues of rat amphiphysin1 (Amph1AB) and mutations of the D*X*F motifs to SGA were used to probe interactions with AP1, AP2, and AP3 complexes in rat brain and COS-7 extracts. *WT*, wild type. *B*, mutational analysis of the FEDNF motif in Amph1AB binding to the AP2 complex. Mutations are made on the background of a functional DPF motif. Longer exposure of the blots confirmed that the limited contribution made by this motif is still functional (data not shown). *C*, mutational analysis of the FDDAF in motif in Amph2AB binding to the AP2 complex. *D*, enhanced binding of amphiphysin1 to the α-adaptin appendage+hinge domain.

mutagenesis presented here confirmed the stronger binding of the F*X*D*X*F motif of amphiphysin to the AP2 adaptor compared with the DPF motif. Therefore, we tested peptides from these regions to measure their affinities directly with purified α-adaptin appendage domain to explain the contribution of individual residues (Fig. 4, *A* and *B*, and Table 1). From our previous work we had found that a 7-mer peptide (**FED**N**F**VP) is sufficient for binding, but residues distant to the motif contribute to binding leading to a 10-fold stronger interaction of the Amph1-DNF 12-mer (INF**FED**N**F**VPEI). This peptide does not bind to the β2-adaptin appendage domain, again confirming our results from pulldown experiments. By mutagenesis we showed that the DPF motif of amphiphysin1 contributes less to binding of AP2 adaptors, and likewise a 12-mer peptide containing this motif (LDLDF**DPF**KPDV) has a lower affinity (~200 μM). Substitution of DNF for DPF in this peptide does not increase the affinity. However, substitution of DPF for DNF in the Amph1-DNF 12-mer reduces the affinity by over 40-fold to about 100 μM, although the peptide still follows the proposed F*X*D*X*F consensus sequence. The reduction is smaller if F*X*DPW is used, where the affinity is 60 μM. The importance of the interaction of the first Phe from F*X*D*X*F motifs was tested by swapping the residues Phe and Glu before the F*X*DNF, and this led to a drop of the affinity to about 180 μM. Exchanging the F*X*DNF to F*X*DDF or F*X*DSF (corresponding to the residues of human synaptojanin1 p170) keeps the affinity below 10 μM, and exchanging to F*X*DAF or F*X*DIF (corresponding to the residues of amphiphysin2 and HIP1, respectively) results in a medium affinity of about 20–30 μM. The F*X*DAF peptide from amphiphysin2 has a similar affinity as the F*X*DNF to DAF exchange in amphiphysin1.

Taken together, the changes of the affinities perfectly match the order we obtained from the pulldown experiments with amphiphysin mutants (Fig. 2, *B* and *C*). All the peptides tested have a stoichiometry of 1:1 except Amph1-DPF 12-mer where two peptides bind to each appendage domain. This peptide contains an overlapping clathrin box (LLDLD) and also contains a version of an F*XX*F motif that can also interact weakly with α-adaptin (7, 11).

Given the different affinities of amphiphysin peptides that all follow the F*X*D*X*F consensus motif, we looked at possible high affinity interaction motifs in other endocytic proteins by sequence comparisons. A 12-mer peptide of the F*X*DLF sequence in Dab2 had a very low affinity. Previously, we found weak affinities for an F*X*DPW peptide from epsin1, and the same applies to an F*X*DPF peptide from Eps15, an F*X*DAF peptide from AP180, and an F*X*DPF peptide from the phospholipase A_2-activating proteins (PLAA). A medium affinity was found for an F*X*DGF peptide from mouse Eps15. However, we know that this is not dependent on the F*X*D*X*F but the overlapping presence of an F*XX*F*XX*L motif (7). Another medium affinity interaction was found for an F*X*DIF from Huntingtin interacting protein 1 (HIP1). Recently, a variation of the F*X*D*X*F α-adaptin-binding motif has been described in the AP180 homolog clathrin assembly lymphoid myeloid leukemia protein (CALM), where the aspartic acid is replaced by a serine (43). We could not detect binding of a corresponding 12-mer peptide to the α-adaptin appendage, but changing the FEDNF in the amphiphysin1 12-mer to FESNF had only a very mild effect leading to a 3-fold decrease in affinity.

Affinities of DX(F/W) Motifs—Many accessory proteins contain multiple copies of D*X*(F/W) and not necessarily a high affinity F*X*D*X*F or W*XX*Φ motif, and some of them are still able

Downloaded from www.jbc.org at MRC Lab of Molecular Biology on October 18, 2008

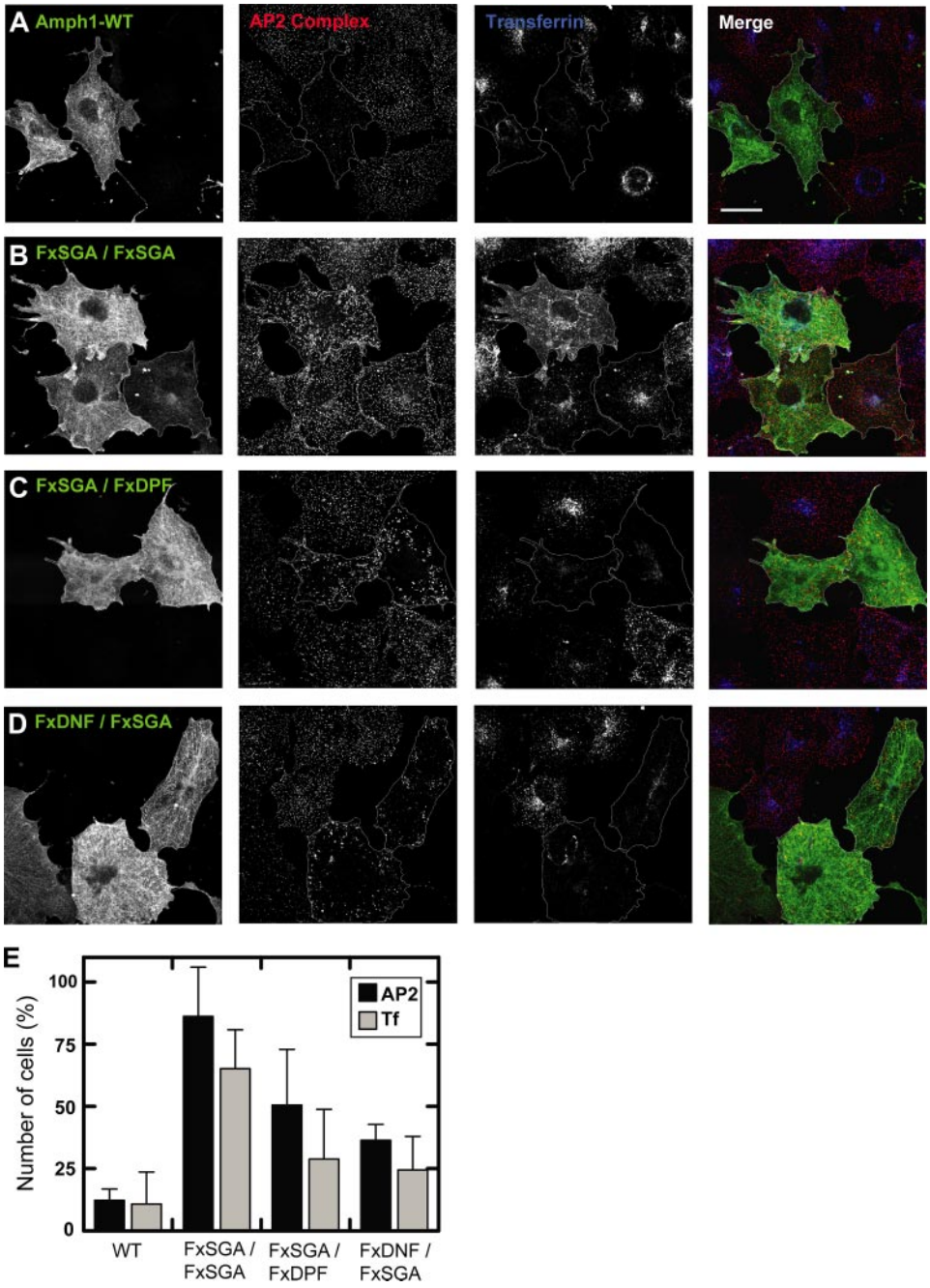

FIGURE 3. **Function of D*X*F motifs *in vivo*.** *A*, full-length amphiphysin1 overexpressed in COS-7 cells (*green*) causes a redistribution of the AP2 puncta (*red*) from the membrane and inhibits uptake of transferrin (*blue*). *B*, double mutant F*X*SGA/F*X*SGA has a small effect on AP2 distribution. *C* and *D*, single SGA mutant of the DPF motif shows a stronger inhibition of the AP2 distribution than the mutant of the DNF motif, consistent with their affinities for AP2 adaptor complexes. *Scale bar*, 10 μm. *E*, quantification of the data for which representative cells are shown in *A–D*. Shown for each transfection are the mean ± S.D. σ*n*-1 for the percentage of transfected cells showing a wild-type AP2 distribution (*black bars*) and wild-type (*WT*) transferrin uptake (*gray bars*). The number of cells quantified for each data point are as follows: WT, 87; F*X*SGA/F*X*SGA, 76; F*X*SGA/F*X*DPF, 148; F*X*DNF/F*X*SGA, 85.

to interact significantly with the α-adaptin appendage. To check whether the affinity of the DPF motif of amphiphysin1 is typical also for other D*X*(F/W) motifs, we measured the binding of several peptides derived from Eps15, epsin1, PLAA, and Dab2 (Fig. 4, *A* and *B*). None of these peptides containing a single D*X*(F/W) motif bound tighter than 200 μM, and the affinities were only slightly greater in the case of double DPF peptides from Eps15 and Dab2. It is worth noting that these peptides bound with a 1:1 stoichiometry to the α-adaptin appendage implying the need for a certain distance between D*X*(F/W) motifs to bind simultaneously to two α-adaptin appendages.

High Resolution Structure—To better understand the interaction between the F*X*D*X*F motif from amphiphysin and the α-adaptin appendage domain, we solved the structure of the core Amph1 F*X*DNF 7-mer peptide bound to the α-adaptin appendage at 1.6 Å resolution. The structure was obtained by soaking the FEDNFVP peptide into a crystal of the α-adaptin appendage in complex with a WV*X*F peptide from synaptojanin (sequence NPKGWVTFEEEE) bound to the side of the sandwich domain. An amphiphysin peptide has previously been crystallized with the α-appendage (7, 8, 12, 18), but our higher resolution allows us to analyze the interaction of the α-adaptin appendage with the peptides in greater detail (Fig. 5). The core of the sandwich subdomain-binding WV*X*F peptide interacts as in the previously published structure (PDB code 1W80 (7)). All residues of the amphiphysin peptide, with the exception of the side chain of Glu, are well resolved in the structure, and all except the Glu and the Pro are involved in the interaction with the α-adaptin appendage. The two bulky side chains of the Phe residues interact with the hydrophobic sites around Trp-840 and Tyr-915, as described previously. The side chain of the Glu corresponding to the first *X* of the F*X*D*X*F is flexible and not visible. This Glu may bond, via a water, to Arg-920 of the α-adaptin appendage, although clearly the side chain is highly flexible. An important interaction for the motif is the salt bridge between the conserved Asp and Arg-916 from the α-adaptin appendage, whereas the interaction with Arg-905 of the α-adaptin appendage determines the specificity for the *X*2 position.

Predictions of Trafficking Proteins That Bind Appendage Domains—Many of the endocytic proteins that bind to adaptors contain multiple copies of D*X*(F/W) motifs clustered in so-called motif domains. Using a specially written computer

Downloaded from www.jbc.org at MRC Lab of Molecular Biology on October 18, 2008

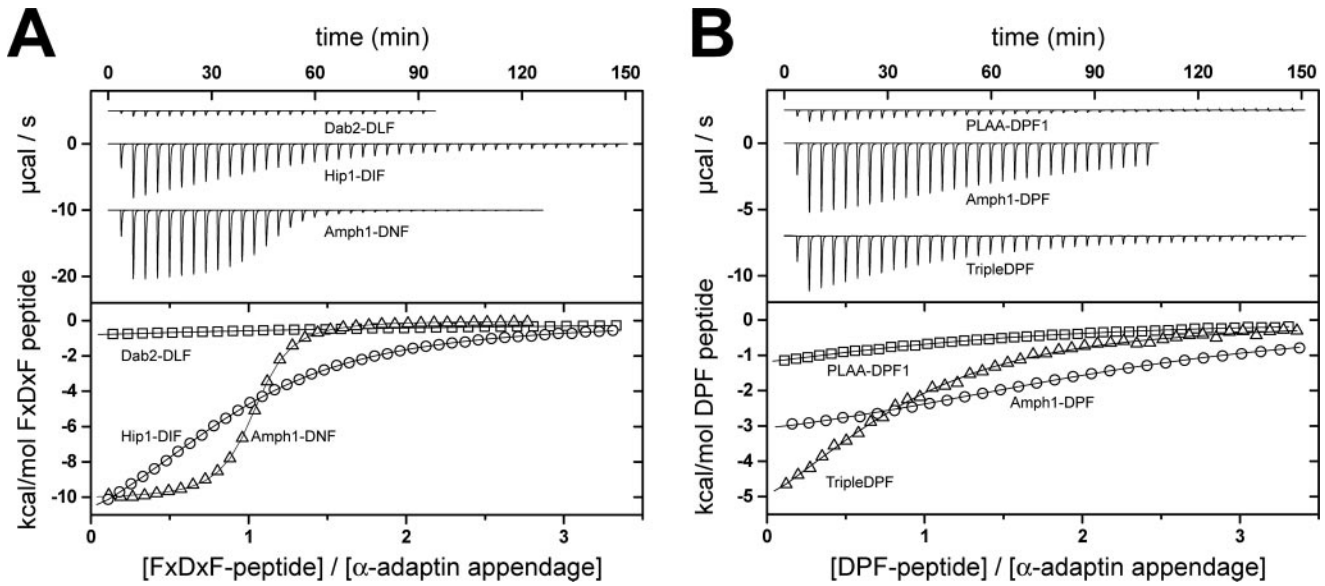

FIGURE 4. **Specificity of F*X* D*X*(F/W) and D*X*(F/W) motifs for the α-adaptin appendage domain.** *A*, profiles of typical calorimetric titrations of Dab2-F*X*DLF, HIP1-F*X*DIF, and Amph1-DNF 12-mer peptides into a solution of the α-adaptin appendage (*upper panel, top* to *bottom*) and the integrated data, normalized to the concentration of the DNF-peptides (*lower panel*). *B*, profiles of typical calorimetric titrations of PLAA-DPF1, Amph1-DPF 12-mer and a triple DPF peptide into a solution of the α-adaptin appendage (*upper panel, top* to *bottom*) and the integrated data, normalized to the concentration of the DNF peptides (*lower panel*). The results of the fits are listed in Table 1.

program (Sequence Motif Search Program),[10] we find that D*X*(F/W) motifs occur more often than expected in human, worm, fly, slime mold, and yeast protein nonredundant data bases. We found that the easiest way to filter the results with confidence was to search for the co-occurrence with other endocytic motifs. A number of other motifs appear in endocytic proteins like the α-adaptin appendage-binding motifs WV*X*F or F*XX*F*XX*(F/L), the clathrin terminal domain-binding motifs LLDLD or PW*XX*W, or the Eps15-homology domain-binding sequence NPF. The program allows the user to search any subset (or even all) of the results for the coincidence of any motifs. For example, a search for a degenerate consensus motif (F(E/D)(D/S)(N/S/D/A/I)F), to look only for high affinity α-adaptin appendage-binding proteins, and the co-occurrence of a DPF motif, leads to about 10 hits in the human data base. As well as the expected appearance of amphiphysin and HIP1, a MAPKKK, a tyrosine kinase, and a Kelch-BTB homolog were also identified. This program[10] will facilitate the search for any novel motif-containing proteins across a wide range of sequenced genomes. This may be of interest to any investigators working in fields where short motifs are important binding determinants.

DISCUSSION

Amphiphysin fulfills a critical function in clathrin-mediated endocytosis by inducing curvature at the neck of a coated pit, while at the same time recruiting the scission molecule dynamin to this position (44). Amphiphysin itself is recruited to sites of endocytosis via its interactions with phospholipids in the plasma membrane (26, 28, 45), with the α-adaptin appendage domain of the AP2 complex (12, 46) and the N-terminal domain of clathrin (5, 47). It contains only two binding motifs for the α-adaptin appendage domain and interacts only weakly with the β2-adaptin appendage domain. This is in contrast to many other endocytic proteins like human Eps15 with 15 DPF, epsin1 with 9 DPW, or AP180 with 4 DPF motifs. Nevertheless, amphiphysin is a major AP2-binding protein (7, 27). Therefore we set out to investigate the molecular basis for the high affinity that the motifs in amphiphysin must have to achieve efficient binding.

In recent crystallization experiments, the platform subdomain of the α-adaptin appendage has been proposed to bind ligands in two different modes. The DP(F/W) motif binds with the Phe or Trp in a large hydrophobic pocket centered around Trp-840. In the second binding mode, F*X*D*X*F motifs bind with the first Phe in the Trp-840 pocket (7, 18). In the first mode the proline will allow the necessary kink in the backbone to allow the Asp to form a hydrogen bond with the backbone of the peptide and also to interact with Arg-905 via a water. A first proposal of this mode of binding would be that the surrounding residues will have very little influence on the binding affinity.

We found that in amphiphysin1 the F*X*D*X*F motif is the major determinant for the interaction with the α-adaptin appendage domain *in vitro* and *in vivo*. This is underscored by the similar affinities of the DNF 12-mer peptide and the construct comprising the N-terminal BAR domain and the motif domain. It also confirms our previous observation that the FEDNF 12-mer peptide but not a FEDPF version blocks clathrin-mediated endocytosis in isolated nerve terminals of bipolar cells (48). The DPF motif is also able to interact with the α-adaptin appendage domain although with an affinity that is at least an order of magnitude weaker than the F*X*D*X*F motif.

The F*X*D*X*F motif was proposed to be responsible for the interactions of other endocytic proteins containing this sequence (7, 13, 18). We showed that this is a strong binding motif for the α-adaptin appendage in amphiphysin1 and the 170-kDa isoform of synaptojanin (7); however, the generali-

[10] H. T. McMahon, personal communication.

Downloaded from www.jbc.org at MRC Lab of Molecular Biology on October 18, 2008

TABLE 1

Binding constants of peptides measured by ITC

Dissociation constants for the interactions of peptides and the α-adaptin appendage as determined by ITC at 10 °C. Note that the dissociation constant K_d is the inverse of the association constant K_a obtained from the binding experiments. The values for ΔH and $T\Delta S$ are given for the association reaction. The experiments marked with an asterisk have been determined previously (7).

Peptide name	sequence	K_d (μM)	ΔH (kcal mol^{-1})	TΔS (kcal mol^{-1})
Amph1-DNF 7mer*	**FEDNF**VP	21	-6.9	-0.8
Amph1-DNF 8mer	**FEDNF**VPE	28	-7.5	-1.6
Amph1-DNF 12mer*	INF**FEDNF**VPEI	2.5	-9.8	-2.5
Amph1-DNF to DPF 12mer	INF**FEDPF**VPEI	100	-6.7	-1.5
Amph1-DNF to DPW 12mer	INF**FEDPW**VPEI	52	-11.1	-5.6
Amph1-DNF 12mer swap	INFE**FDNF**VPEI	180	-7.7	-2.8
Amph1-DNF to DDF 12 mer	INF**FEDDF**VPEI	3.7	-10.2	-3.1
Amph1-DNF to DSF 12 mer	INF**FEDSF**VPEI	5.4	-10.6	-3.7
Amph1-DNF to DAF 12mer	INF**FEDAF**VPEI	21	-6.5	-0.4
Amph1-DNF to DIF 12mer	INF**FEDIF**VPEI	29	-8.7	-2.8
Amph1-DNF to SNF 12mer	INF**FESNF**VPEI	7.4	-10.1	-3.5
Amph1-FKDNF 12mer	INF**FKDNF**VPEI	4.4	-11.8	-4.8
Amph2-DAF 12mer	LSLF**DDAF**VPEI	12	-9.4	-3.0
Amph1-DPF 12mer	LDLDF**DPF**KPDV	190	-4.4	0.4
Amph1-DPF to DNF	LDLDF**DNF**KPDV	> 300		
Syjn-FKDSF*	LDG**FKDSF**DLQG	27	-14.3	-8.4
Syjn-FEDNF*	LDG**FEDNF**DLQS	4.5	-11.9	-5.0
Dab2-FxDLF	QSN**FLDLF**KGNA	> 300		
Eps15-FxDPF	**DMFCDPF**TSST	> 300		
Eps15-FxDGF*	**SFGDGF**ADFSTL	140	-12.7	-5.5
Eps15-FxGGF*	**SFGGGF**ADFSTL	120	-14.0	-4.6
AP180-FxDAF	I**DLFGDAF**GSSA	> 300		
Epsin1-FxDPW*	APA**FSDPW**GGSP	200	-10.0	-5.2
PLAA-FxDPF	NPS**FSDPF**TGGG	250	-3.2	1.4
Hip1-FxDIF	DNK**FDDIF**GSSF	94	-14.7	-9.5
CALM-FxSVF	NVD**FESVF**GNKS	> 300		
TripleDPF	**DPF**KD**DPF**VGS**DPF**	96	-8.2	-2.9
Dab2-DPF	PNP**DPF**RD**DPF**AQP	250	-14.4	-9.7
Eps15-double	TST**DPF**TTSST**DPF**SAS	140	-8.2	-3.2
Eps15-DCF	PFAS**DCF**FKQT	> 300		
Epsin-DPW	GPPSS**DPW**APAP	> 300		
PLAA-DPW	YNTSD**DPW**LTAY	> 300		
PLAA-DPF1	TLPTA**DPF**TGAG	290	-2.4	2.2
PLAA-DPF2	TMAGV**DPF**TGNS	230	-2.4	2.3
GAK-DPFDQF	TV**DPFDQF**LLPS	240	-4.7	0.0
GAK-DLF	KP**DLF**GEFLNSD	> 300		

zation does not hold true for many other proteins such as Dab2, Eps15, AP180, and epsin1. In fact, by mutating this motif in the motif domain of amphiphysin1 and by titrations of peptides with different variants of this motif, we found that the fourth residue in the F*X*D*X*F motif is critical for a high affinity interaction. The interaction of this residue with the α-adaptin appendage is strong with residues like Asn, Ser, and Asp. These residues are found in motifs from amphiphysin1 and the 170-kDa isoform of synaptojanin, which have a high affinity because they can interact with the side chain of Arg-905 of the α-adaptin appendage. Small residues like Ala and Ile are also tolerated and give rise to a medium affinity, such as that observed in amphiphysin2 and HIP1. Other residues like Val or Leu weaken the interaction

Downloaded from www.jbc.org at MRC Lab of Molecular Biology on October 18, 2008

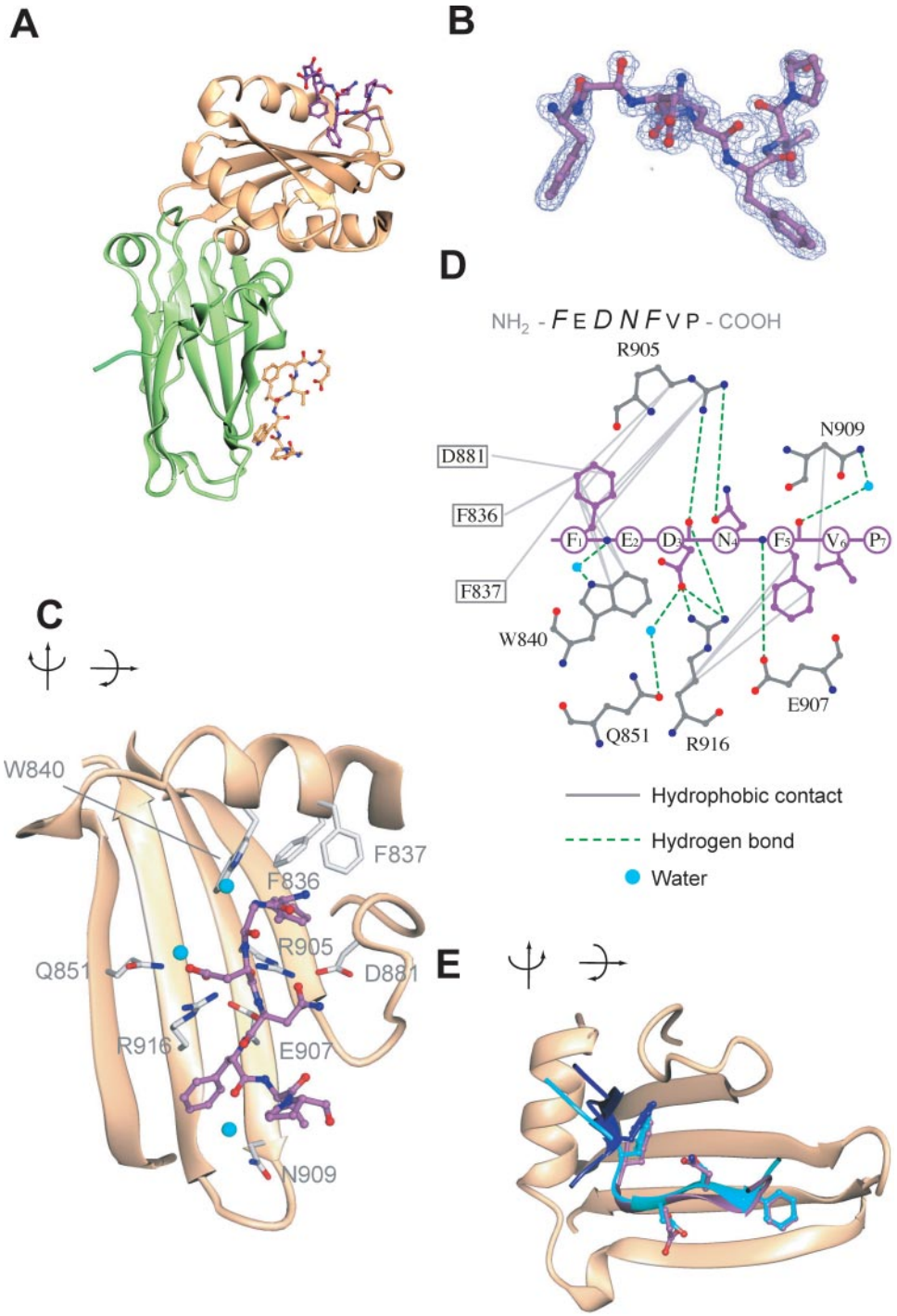

FIGURE 5. **High resolution structure of F*X*D*X*F peptide with the α-adaptin appendage domain.** *A*, ribbon diagram of the 1.6 Å structure of the α-adaptin appendage with the W*XX*F peptide from synaptojanin bound to the side of the sandwich subdomain (*green*) and the FEDNFVP 7-mer peptide from amphiphysin1 bound to the platform subdomain (*gold*). *B*, density for the amphiphysin peptide. All residues can be clearly seen, with the exception of the Glu, as discussed in the text. *C*, details of the F*X*D*X*F peptide-binding sites showing interacting α-adaptin appendage residues and coordinated waters (*blue*) involved in binding. *D*, FEDNFVP peptide displayed as a linear chain showing hydrogen bonding and ionic interactions (*dashed green lines*) and hydrophobic interactions (*gray lines*). The most important peptide residues are in *italics*. *E*, comparison of the modes of binding of the synaptojanin FKDSF motif (*cyan*) (PDB code 1W80), the amphiphysin FEDNF (*purple*, this work), and a DPW from epsin (*blue*) (PDB code 1KYD).

such that the affinity is similar to a standard DP(F/W) motif. The results were confirmed in titration experiments using F*X*D*X*F peptides from different proteins (Table 1). The weak F*X*D*X*F motifs have affinities in the same range as isolated DP(F/W) motifs and may well contribute to binding when they are clustered together like in AP180, CALM, or Dab2 (12, 43, 49) or combined with a β-sandwich-binding motif like in connecdenn (21).

In our and other's structural work the *X*2 residues function as acceptors for a hydrogen bond from Arg-905 (7, 18). The interaction with an F*X*DDF could even increase the contribution from this position by ionic attraction. It is not clear, however, why Ile is tolerated at this position but Val and Leu are not.

The first *X* in the F*X*D*X*F is very flexible in our structure, indicating looser requirements here. It may be possible that the Glu of FEDNF motifs bonds via a water to Arg-920 of the α-adaptin appendage, which is not possible for the FKDSF from human synaptojanin which was used in our previous structure.

The Asp at the third position of the F*X*D*X*F motif is highly conserved. However, recent data by Meyerholz *et al.* (43), as well as our Amph1 F*X*SNF peptide, show that a hydrogen bonding partner like Ser is sufficient for binding to Arg-916 from the α-adaptin appendage in certain contexts.

In the case of the F*X*DPW motifs of epsin1, PLAA, and the FEDPW version of the amphiphysin peptide, the precise binding mode has not been conclusively resolved by our study, and further structural data are needed to clarify whether they adopt the extended F*X*D*X*F or the DP(F/W) loop conformation. Certainly, we conclude from this that there are different modes of binding centered at the large hydrophobic pocket on the α-adaptin appendage involving Phe-836, Phe-837, and Trp-840 with the surrounding charged and hydrophobic residues influencing the strength of the interactions.

We conclude that F*X*D*X*F is not a general high affinity binding motif for α-adaptin but that certain residues at the fourth position are favorable for binding (Asn, Ser, Ala, Ile, and Asp) and that additional determinants in the surrounding residues

Downloaded from www.jbc.org at MRC Lab of Molecular Biology on October 18, 2008

contribute as well. Therefore, the core consensus sequence for a medium to high affinity binding motif for the α-adaptin appendage is F(E/D)(D/S)(N/S/D/A/I)F.

The affinity of the DNF 12-mer from amphiphysin1 explains how this protein can be a major ligand for the AP2 complex, although it contains only two binding motifs, especially when amphiphysin dimers bind to clustered AP2 in assembly zones. Therefore, by predicting endocytic proteins only on the basis of having multiple D*X*(F/W) motifs, we would have missed such proteins. If D*X*(F/W) motifs are simply a means of ensuring recruitment to an adaptor complex, then one high affinity motif will substitute for multiple low affinity motifs, which will work rather like Velcro (8, 9, 44). Together with the WV*X*F motif binding to the side of the β-sandwich subdomain and the still unidentified binding site for the F*XX*F*XX*L motif, the α-adaptin appendage domain is able to interact with up to four different types of motifs.

Recently, it has been reported that the N-terminal region of NECAP also interacts with F*X*D*X*F motifs with a similar affinity to the α-adaptin appendage (50). The structure of this domain revealed that it belongs to the pleckstrin homology domain superfamily, but the lipid-binding residues are not conserved. The relative affinities for F*X*D*X*F motifs from several endocytic proteins showed that the NECAP PHear binding consensus sequence differs from that of α-adaptin appendage domain. Because NECAP also interacts strongly with the side site of the α-adaptin appendage domain via its C-terminal WV*X*F motif, they may indeed serve as a third appendage domain of the AP2 complex.

Short sequence motifs occurring in repeats also play a role in other trafficking pathways. Well studied examples are the FG motifs of nuclear pore proteins, often placed in FSFG or GLFG motifs, which interact with cargo carriers (51–53). Similarly, F*XX*Φ motifs have been shown to interact with γ-appendage domains in the AP1 complex and GGA proteins (11, 14, 54). Many endocytic proteins, including epsin, CALM, stonin2, and Dab2, have NPF motifs that mediate the interaction with Eps15 homology domains of proteins like Eps15 and intersectin (55, 56). In contrast to single high affinity motifs such as phospho-Y*XX*Φ motifs binding to SH2 domains, NP*X*Y motifs binding to PTB domains, or the F*X*D*X*F or WV*X*F for the α-adaptin appendage discussed here, a chain of repeated low affinity sequences offers additional mechanisms for regulation. They can sample density of binding partners using avidity effects, and by placing other types of binding motifs (*e.g.* for clathrin) into the repeat they can interact with different binding partners in a cooperative or exclusive manner depending on the number, the sequential order, and the spacing of the motifs (5, 7, 8, 18, 22, 24). We and others have shown that the same mechanism is also used in AP1- and GGA-dependent trafficking from the Golgi, where F*XX*(F/W) motifs interact with the γ- and GGA-appendage domains (11, 14, 16, 57–59).

A further level of complexity is added by the fact that several α- or γ-appendage-binding proteins also interact with the β1- and β2-adaptin appendage domains, which are also present in the AP1 and AP2 complexes (7, 8, 11, 17, 24, 60, 61). Because the binding sites on the appendage domains and the binding motifs are at least partially overlapping, the affinity, copy number, and the relative position of the motifs determine the specific recruitment of an accessory protein to a clathrin-coated pit. Amphiphysin is the major recruiter of dynamin to the neck of a clathrin-coated pit at the plasma membrane and is specific for the α-adaptin appendage only. There should be other proteins taking over this function at the Golgi. Good candidates are sorting nexin 9 and the pacsins, which, like amphiphysin, contain BAR domains for membrane interactions and SH3 domains for dynamin recruitment.

Acknowledgments—We thank our laboratory members for fruitful discussions.

REFERENCES

1. Pearse, B. M., and Robinson, M. S. (1984) *EMBO J.* **3,** 1951–1957
2. Ahle, S., and Ungewickell, E. (1986) *EMBO J.* **5,** 3143–3149
3. Ford, M. G., Pearse, B. M., Higgins, M. K., Vallis, Y., Owen, D. J., Gibson, A., Hopkins, C. R., Evans, P. R., and McMahon, H. T. (2001) *Science* **291,** 1051–1055
4. Fotin, A., Cheng, Y., Sliz, P., Grigorieff, N., Harrison, S. C., Kirchhausen, T., and Walz, T. (2004) *Nature* **432,** 573–579
5. Miele, A. E., Watson, P. J., Evans, P. R., Traub, L. M., and Owen, D. J. (2004) *Nat. Struct. Mol. Biol.* **11,** 242–248
6. Dell'Angelica, E. C. (2001) *Trends Cell Biol.* **11,** 315–318
7. Praefcke, G. J., Ford, M. G., Schmid, E. M., Olesen, L. E., Gallop, J. L., Peak-Chew, S. Y., Vallis, Y., Babu, M. M., Mills, I. G., and McMahon, H. T. (2004) *EMBO J.* **23,** 4371–4383
8. Schmid, E. M., Ford, M. G., Burtey, A., Praefcke, G. J., Peak-Chew, S. Y., Mills, I. G., Benmerah, A., and McMahon, H. T. (2006) *PLoS Biol.* **4,** e262
9. Schmid, E. M., and McMahon, H. T. (2007) *Nature* **448,** 883–888
10. Collins, B. M., McCoy, A. J., Kent, H. M., Evans, P. R., and Owen, D. J. (2002) *Cell* **109,** 523–535
11. Mills, I. G., Praefcke, G. J., Vallis, Y., Peter, B. J., Olesen, L. E., Gallop, J. L., Butler, P. J., Evans, P. R., and McMahon, H. T. (2003) *J. Cell Biol.* **160,** 213–222
12. Owen, D. J., Vallis, Y., Noble, M. E., Hunter, J. B., Dafforn, T. R., Evans, P. R., and McMahon, H. T. (1999) *Cell* **97,** 805–815
13. Mishra, S. K., Hawryluk, M. J., Brett, T. J., Keyel, P. A., Dupin, A. L., Jha, A., Heuser, J. E., Fremont, D. H., and Traub, L. M. (2004) *J. Biol. Chem.* **279,** 46191–46203
14. Mattera, R., Ritter, B., Sidhu, S. S., McPherson, P. S., and Bonifacino, J. S. (2004) *J. Biol. Chem.* **279,** 8018–8028
15. Ritter, B., Philie, J., Girard, M., Tung, E. C., Blondeau, F., and McPherson, P. S. (2003) *EMBO Rep.* **4,** 1089–1095
16. Wasiak, S., Denisov, A. Y., Han, Z., Leventis, P. A., de Heuvel, E., Boulianne, G. L., Kay, B. K., Gehring, K., and McPherson, P. S. (2003) *FEBS Lett.* **555,** 437–442
17. Owen, D. J., Vallis, Y., Pearse, B. M., McMahon, H. T., and Evans, P. R. (2000) *EMBO J.* **19,** 4216–4227
18. Brett, T. J., Traub, L. M., and Fremont, D. H. (2002) *Structure* (*Lond.*) **10,** 797–809
19. Kalthoff, C., Alves, J., Urbanke, C., Knorr, R., and Ungewickell, E. J. (2002) *J. Biol. Chem.* **277,** 8209–8216
20. Hinrichsen, L., Meyerholz, A., Groos, S., and Ungewickell, E. J. (2006) *Proc. Natl. Acad. Sci. U. S. A.* **103,** 8715–8720
21. Allaire, P. D., Ritter, B., Thomas, S., Burman, J. L., Denisov, A. Y., Legendre-Guillemin, V., Harper, S. Q., Davidson, B. L., Gehring, K., and McPherson, P. S. (2006) *J. Neurosci.* **26,** 13202–13212
22. Jha, A., Agostinelli, N. R., Mishra, S. K., Keyel, P. A., Hawryluk, M. J., and Traub, L. M. (2004) *J. Biol. Chem.* **279,** 2281–2290
23. Walther, K., Diril, M. K., Jung, N., and Haucke, V. (2004) *Proc. Natl. Acad. Sci. U. S. A.* **101,** 964–969
24. Edeling, M. A., Mishra, S. K., Keyel, P. A., Steinhauser, A. L., Collins, B. M., Roth, R., Heuser, J. E., Owen, D. J., and Traub, L. M. (2006) *Dev. Cell* **10,** 329–342

Downloaded from www.jbc.org at MRC Lab of Molecular Biology on October 18, 2008

25. Tebar, F., Sorkina, T., Sorkin, A., Ericsson, M., and Kirchhausen, T. (1996) *J. Biol. Chem.* **271,** 28727–28730
26. Peter, B. J., Kent, H. M., Mills, I. G., Vallis, Y., Butler, P. J., Evans, P. R., and McMahon, H. T. (2004) *Science* **303,** 495–499
27. Wigge, P., Kohler, K., Vallis, Y., Doyle, C. A., Owen, D., Hunt, S. P., and McMahon, H. T. (1997) *Mol. Biol. Cell* **8,** 2003–2015
28. Razzaq, A., Robinson, I. M., McMahon, H. T., Skepper, J. N., Su, Y., Zelhof, A. C., Jackson, A. P., Gay, N. J., and O'Kane, C. J. (2001) *Genes Dev.* **15,** 2967–2979
29. Lee, E., Marcucci, M., Daniell, L., Pypaert, M., Weisz, O. A., Ochoa, G. C., Farsad, K., Wenk, M. R., and De Camilli, P. (2002) *Science* **297,** 1193–1196
30. Wiseman, T., Williston, S., Brandts, J. F., and Lin, L. N. (1989) *Anal. Biochem.* **179,** 131–137
31. Leslie, A. W. G. (1992) *Joint CCP4 and ESF-EACMB Newsletter on Protein Crystallography,* Vol. 26, Daresbury Laboratory, Warrington, UK
32. Collaborative Computational Project, Number 4 (1994) *Acta Crystallogr. Sect. D Biol. Crystallogr.* **50,** 760–763
33. Emsley, P., and Cowtan, K. (2004) *Acta Crystallogr. Sect. D. Biol. Crystallogr.* **60,** 2126–2132
34. Jones, T. A., Zou, J. Y., Cowan, S. W., and Kjeldgaard, M. (1991) *Acta Crystallogr. Sect. A* **47,** 110–119
35. Murshudov, G. N., Vagin, A. A., and Dodson, E. J. (1997) *Acta Crystallogr. Sect. D Biol. Crystallogr.* **53,** 240–255
36. Berman, H. M., Westbrook, J., Feng, Z., Gilliland, G., Bhat, T. N., Weissig, H., Shindyalov, I. N., and Bourne, P. E. (2000) *Nucleic Acids Res.* **28,** 235–242
37. Wallace, A. C., Laskowski, R. A., and Thornton, J. M. (1995) *Protein Eng.* **8,** 127–134
38. Slepnev, V. I., Ochoa, G. C., Butler, M. H., and De Camilli, P. (2000) *J. Biol. Chem.* **275,** 17583–17589
39. Ford, M. G., Mills, I. G., Peter, B. J., Vallis, Y., Praefcke, G. J., Evans, P. R., and McMahon, H. T. (2002) *Nature* **419,** 361–366
40. Tebar, F., Bohlander, S. K., and Sorkin, A. (1999) *Mol. Biol. Cell* **10,** 2687–2702
41. Haffner, C., Di Paolo, G., Rosenthal, J. A., and De Camilli, P. (2000) *Curr. Biol.* **10,** 471–474
42. Wigge, P., Vallis, Y., and McMahon, H. T. (1997) *Curr. Biol.* **7,** 554–560
43. Meyerholz, A., Hinrichsen, L., Groos, S., Esk, P. C., Brandes, G., and Ungewickell, E. J. (2005) *Traffic* **6,** 1225–1234
44. Praefcke, G. J., and McMahon, H. T. (2004) *Nat. Rev. Mol. Cell Biol.* **5,** 133–147
45. Takei, K., Slepnev, V. I., Haucke, V., and De Camilli, P. (1999) *Nat. Cell Biol.* **1,** 33–39
46. David, C., McPherson, P. S., Mundigl, O., and De Camilli, P. (1996) *Proc. Natl. Acad. Sci. U. S. A.* **93,** 331–335
47. McMahon, H. T., Wigge, P., and Smith, C. (1997) *FEBS Lett.* **413,** 319–322
48. Jockusch, W. J., Praefcke, G. J., McMahon, H. T., and Lagnado, L. (2005) *Neuron* **46,** 869–878
49. Morris, S. M., and Cooper, J. A. (2001) *Traffic* **2,** 111–123
50. Ritter, B., Denisov, A. Y., Philie, J., Allaire, P. D., Legendre-Guillemin, V., Zylbergold, P., Gehring, K., and McPherson, P. S. (2007) *EMBO J.* **26,** 4066–4077
51. Bayliss, R., Littlewood, T., Strawn, L. A., Wente, S. R., and Stewart, M. (2002) *J. Biol. Chem.* **277,** 50597–50606
52. Iovine, M. K., Watkins, J. L., and Wente, S. R. (1995) *J. Cell Biol.* **131,** 1699–1713
53. Radu, A., Moore, M. S., and Blobel, G. (1995) *Cell* **81,** 215–222
54. Lui, W. W., Collins, B. M., Hirst, J., Motley, A., Millar, C., Schu, P., Owen, D. J., and Robinson, M. S. (2003) *Mol. Biol. Cell* **14,** 2385–2398
55. Salcini, A. E., Confalonieri, S., Doria, M., Santolini, E., Tassi, E., Minenkova, O., Cesareni, G., Pelicci, P. G., and Di Fiore, P. P. (1997) *Genes Dev.* **11,** 2239–2249
56. de Beer, T., Carter, R. E., Lobel-Rice, K. E., Sorkin, A., and Overduin, M. (1998) *Science* **281,** 1357–1360
57. Collins, B. M., Praefcke, G. J., Robinson, M. S., and Owen, D. J. (2003) *Nat. Struct. Biol.* **10,** 607–613
58. Miller, G. J., Mattera, R., Bonifacino, J. S., and Hurley, J. H. (2003) *Nat. Struct. Biol.* **10,** 599–606
59. Burman, J. L., Wasiak, S., Ritter, B., de Heuvel, E., and McPherson, P. S. (2005) *FEBS Lett.* **579,** 2177–2184
60. Lundmark, R., and Carlsson, S. R. (2002) *Biochem. J.* **362,** 597–607
61. Mishra, S. K., Keyel, P. A., Edeling, M. A., Dupin, A. L., Owen, D. J., and Traub, L. M. (2005) *J. Biol. Chem.* **280,** 19270–19280

Downloaded from www.jbc.org at MRC Lab of Molecular Biology on October 18, 2008

Supplemental Information

Data Collection Statistics

Collected	Station 9.6 SRS Daresbury
Spacegroup	C2
Cell (a b c (Å) α β γ (˚))	144.51 66.98 39.73 90 94.91 90
Resolution (Å) (outer bin)	72.54 – 1.6 (1.69 – 1.60)
Completeness (%)	96.3 (89.2)
Multiplicity	2.7 (2.4)
Mean Intensity (I)	12250 (965)
Sigma (σ)	2106.8 (510.9)
I / σ	5.8 (1.9)
Wilson Plot B ($Å^2$)	17.59
R_{merge}	0.075 (0.372)
R_{meas}	0.091 (0.463)

Refinement Statistics

R (%)	18.1
R_{Free} (%)	20.7
Test set size (%)	5.1
<B> $Å^2$ (mean, overall)	16.3
$N_{reflections}$ (N_{free})	45466 (2427)
N_{atoms} (N_{water})	5364 (463)
rms deviation from ideality	
Bond lengths (Å)	0.011
Bond angles (˚)	1.3
Ramachandran violations	0